Pure Appl. Geophys.

https://doi.org/10.1007/s00024-017-1763-z

Pure and Applied Geophysics

S-to-P Conversions from Mid-mantle Slow Scatterers in Slab Regions: Observations of Deep/Stagnated Oceanic Crust?

Xiaobo He[1] and Yixian Zheng[1]

Abstract—The fate of a subducted slab is a key ingredient in the context of plate tectonics, yet it remains enigmatic especially in terms of its crustal component. In this study, our efforts are devoted to resolve slab-related structures in the mid-mantle below eastern Indonesia, the Izu–Bonin region, and the Peru area by employing seismic array analysing techniques on high-frequency waveform data from F-net in Japan and the Alaska regional network and the USArray in North America. A pronounced arrival after the direct P wave is observed in the recordings of four deep earthquakes (depths greater than 400 km) from three subduction systems including the Philippines, the Izu–Bonin, and the Peru. This later arrival displays a slightly lower slowness compared to the direct P wave and its back-azimuth deviates somewhat from the great-circle direction. We explain it as an S-to-P conversion at a deep scatterer below the sources in the source region. In total, five scatterers are seen at depths ranging from ~930 to 1500 km. Those scatterers appear to be characterised by an ~7 km-thick low-velocity layer compared to the ambient mantle. Combined evidence from published mineral physical analysis suggests that past subducted oceanic crust, possibly fragmented, is most likely responsible for these thin-layer compositional heterogeneities trapped in the mid-mantle beneath the study regions. Our observations give a clue to the potential fate of subducted oceanic crust.

Key words: Oceanic crust, Mid-mantle, Subduction zone, S-to-P conversion, Seismic array.

1. Introduction

Our current understanding of the fate of subducted oceanic slabs has largely benefitted from seismic tomography, which has been very successful in exploring the large-scale structure of the interior of the Earth (e.g., Dziewonski and Woodhouse 1987; French and Romanowicz 2015). Tomographic efforts have led to a picture that slabs exhibit a range of behaviours including slabs stagnant in the transition zone, slabs trapped in the uppermost lower mantle, and slabs penetrating well into the lower mantle, perhaps, even to the base of the mantle (e.g., Fukao and Obayahi 2013). Seismic tomography cannot, however, resolve the small-scale structures related to mid-ocean-ridge-basalt (MORB) component separated from the underlying lithosphere. Such small-scale heterogeneities in the mantle can give important insight into the dynamics and composition of the Earth's interior (e.g., Helffrich 2006; Rost et al. 2008; Bentham and Rost 2014; Kaneshima 2016). This significance stimulates us to detect those chemically distinct structures in the deep mantle by employing seismic array techniques on high-frequency data (e.g., Rost and Thomas 2002).

The previous studies have demonstrated that small-scale heterogeneity spreads throughout the Earth's mantle (e.g., Hedlin et al. 1997), in particular in the uppermost lower mantle by analysing scattered energy arriving in the P coda (e.g., Kaneshima 2003, 2009; Korenaga 2015), and in the base of mantle by inferring from PKP precursors (e.g., Waszek et al. 2015) and PKKP precursors (e.g., Mancinelli and Shearer 2016). Mid-mantle heterogeneities beneath subduction zones have been resolved by S-to-P converted wave, which starts as a down-going S wave, converted to a P energy at the small-scale structure below sources, and received at a seismic array (e.g., Castle and van der Hilst 2003; Niu et al. 2003; Vanacore et al. 2006; Li et al. 2014; Niu 2014; Yang and He 2015). This converted energy, perhaps, offers the most direct signal to reflect the small-scale structures in the mid-mantle,

Electronic supplementary material The online version of this article (https://doi.org/10.1007/s00024-017-1763-z) contains supplementary material, which is available to authorised users.

[1] Department of Marine Sciences, Ocean College, Zhejiang University, Zhoushan 316000, China. E-mail: xbhe@zju.edu.cn

Published online: 03 February 2018

and its analysis suggests a clear link between the seismic scatterers with a distinctly compositional layer tightly related to subducted oceanic crust in the Japan subduction zone (e.g., Niu 2014).

In this study, we systematically search the small-scale scatterers beneath the subduction zones of the Philippines, Izu–Bonin, and Peru by analysing broad-band S-to-P waveform data from F-net in Japan and the regional Alaska network and USArray in North America, respectively, and investigate the possible connection between deep, short-wavelength compositional heterogeneities and subduction processes, as well as understand the plausible seismic properties of detected scatterers in the deep mantle below three subduction systems.

2. *Data and Analysis*

We visually inspected record sections from all events with magnitude greater than 5.8 and depth deeper than 300 km recorded at F-net in Japan and the regional seismic network in Alaska (AK) as well as USArray (TA). As a result, a total of four record sections containing pronounced SdP arrivals are collected, providing the precious information to explore the mantle heterogeneities. Selected events occurred beneath the subduction zones of Philippines, Izu–Bonin, and Peru. The information for all events is presented in Table 1. Figure 1 shows paths from Sunda to F-net, Izu–Bonin to AK, and Peru to AK. The distributions of all collected events for searching for conspicuous SdP phases are presented in Fig. S1 of supplementary materials. A two-pass, two-pole butterworth bandpass filter with corner frequency at 0.05 and 0.5 Hz is applied to the raw data. Array analysis techniques including 4th root vespagram and beam-forming analysis (e.g., Rost and Thomas 2002) are employed to constrain the slowness and azimuth of SdP. The slowness is varying between − 1 and 1 s/deg^{-1} (relative to P) with an increment of 0.1 s/deg^{-1} to produce vespagrams. In addition, 1D synthetic waveforms via a propagation-matrix algorithm (Wang 1999) based on a slightly modified IASPEI91 model (Kennett and Engdahl 1991) (i.e., assuming a horizontal reflector) in light of previous studies (e.g., Niu et al. 2003) are produced to improve our understanding of the arrivals and related small-scale structures in the mid-mantle. Specifically, a 7 km-thick LVL, in which shear-wave velocity and density change by − 4 and 5%, respectively, is constructed and embedded below sources for simulation (see an example in Fig. 1e). The attenuation structure in the whole crust and mantle for simulations is presented in Figure S2 of supplementary materials, and source mechanisms for four events are taken from the Harvard CMT solutions. It is worth mentioning that a dipping structure can affect SdP amplitude, the discrepancy in amplitude between synthetics and data can hence be partly due to an uncertain dipping geometry. In addition, a dipping geometry is thought to have influences on S-to-P slowness. However, our 1-D modelling turns out to adequately explain the observed slowness, which, in turn, suggests that the dipping angle is small here, although it is difficult to constrain preciously.

We plot record sections to demonstrate the primary arrivals (e.g., P, pP, sP, etc.) together with their coda. All traces are aligned along the first arrival P wave in the profiles. Here, we observe a conspicuous later arrival after the direct P wave, and name it as SdP (source-sided S-to-P conversion wave), which starts as a down-going S wave and subsequently converts to P wave at a scatterer below sources

Table 1

Earthquakes used here and observations of SdP in addition to scatterer location

Event Date	Lat.	Lon.	Depth (km)	Mag.	Scatterers depth (km) & Location	Network
2005-02-05	5.29N	123.33E	525	7.1	950 2.89N 122.40E	F-net
2007-07-21	8.13S	71.27W	644.9	6.1	1150 13S 67.69W	TA
2007-07-21	8.13S	71.27W	644.9	6.1	1500 18S 63.29W	TA
2010-07-23	6.49N	123.48E	578	7.6	930 4.29N 122.7E	F-net
2015-06-23	27.73N	139.73E	460	6.5	1020 25.49N 137.9E	AK

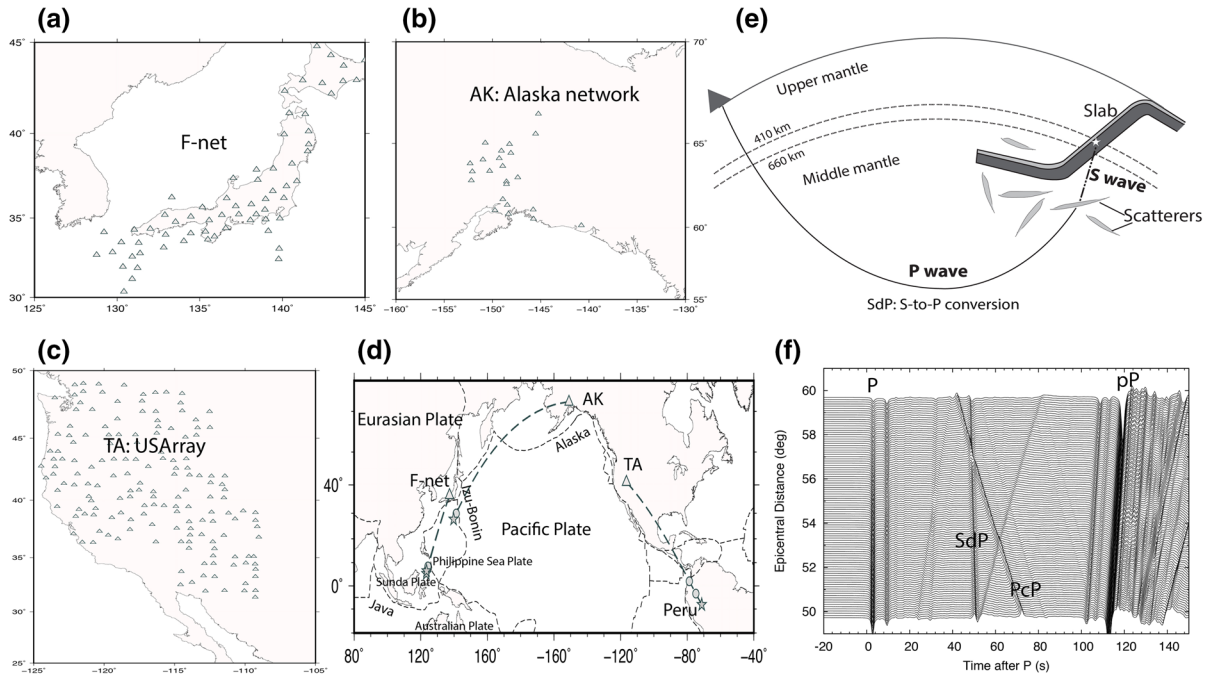

Figure 1

Distribution of stations (**a** F-net, **b** Alaska network (AK), and **c** USArray (TA)) and events (see Table 1 for details) along with great-circle path defined by source(stars)-array(triangles) pair (**d**), and the circles denote the locations of detected scatterers and the real locations are slightly off from the great-circle direction as seen from beam-form analyses. Upper right (**e**) is a schematic figure depicting the geometric ray paths for S-to-P conversion (SdP). A synthetic section (**f**) comprising P and SdP is produced according to a slightly modified IASPEI91 model; here, the source roots at 600 km depth and S-to-P converts from 1100 km depth

(Fig. 1). Our analysis reveals that this SdP exhibits slightly lower slowness compared to P wave, and its back-azimuth deviates from the great-circle direction by less than four degrees, which have been determined by slowness-back-azimuth beam-forming (Fig. 2). It is worth noting that slowness and back-azimuth deviations can be jointly constrained by beam-forming analysis (e.g., Rost and Thomas 2002). For comparison, the vespagrams for the synthetic SdP waves are also presented (e.g., Fig. 4d). The signatures of the later arrival here are similar with those of previously observed signals in other subduction zones (e.g., Vanacore et al. 2006; Niu 2014; Yang and He 2015).

The target wave displays slightly lower slowness and late arrival compared to P wave. Introducing an S-wave segment along the ray-path can readily explain both slowness and arrival-time characteristics. To further discriminate that this arrival is a product of S-to-P conversion or P-to-P reflection from a scatterer, we conduct waveform modelling, but exclude down-going SV waves to the simulation for the 2010 July 23 event (Fig. 3). The synthetic section of excluding the down-going SV waves demonstrates no SdP arrival, whereas the existing SdP for the full wave-fields modelling. The synthetic calculation hence further indicates a S-to-P conversion rather than P-to-P reflection.

To determine the scatterer location, we first constrain its depth according to differential travel-times between P and SdP by try and error, and then conduct a 1-D ray-tracing to constrain its location (longitude and latitude). Both analyses are based on a variety of perturbed IASP91 models.

3. *Results*

In this study, a total of five scatterers are detected by searching our data set. The constrained depths of mid-mantle scatterers, summarised in Table 1, display a wide spectrum of depths ranging from

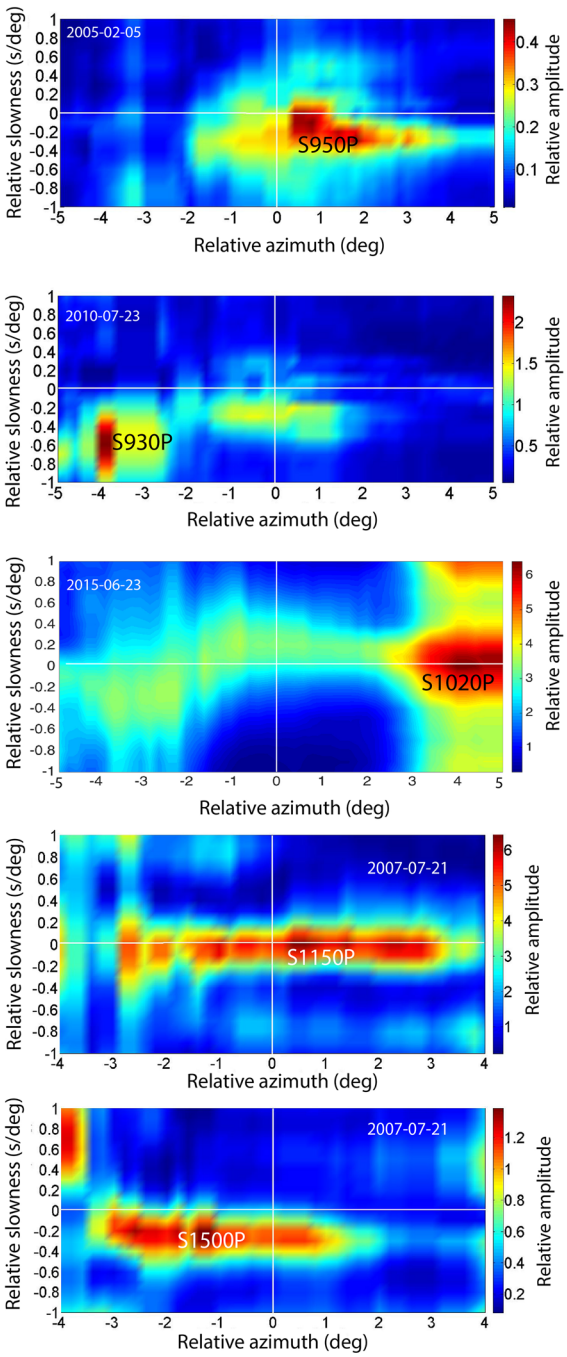

Figure 2
Beam-forming analysing results for the four events data, and the S-to-P conversion occurs slightly out of great-circle-plane. For comparison, the same analyses for the direct P waves are presented in the Fig. S3 of supplementary materials, which demonstrates that the P-wave energies predominantly come from the great-circle directions

~930–1500 km near the source areas. The determined locations of out-of-plane scatterers are also presented in Table 1. Here, we describe our observations from west to east for the three subduction zones.

3.1. Eastern Indonesia

This region is characterised by the subduction of the Philippine Sea Plate beneath the Sunda Plate. Here, two scatterers at depths of ~950 km (Fig. 4) and ~930 km (Fig. 5) are seen from analysing F-net data in this region. Both SdP arrivals slightly deviate from the great-circle direction defined by the source and the station by less than 4° as determined by the beam-forming analyses (Fig. 2).

3.2. The Izu–Bonin Region

The Izu–Bonin–Mariana system formed as a result of subduction of the western Pacific Plate beneath the Philippine Sea Plate. We detect one scatterer at ~1020 km depth (Fig. 6) in this region from analysing the waveform data of one deep event beneath the Izu–Bonin zone recorded at the regional seismic network in Alaska. The record section exhibits noticeable SdP arrivals, which are adequately reproduced by the waveform simulations (Fig. 6). Regional P-wave tomography images do show high-speed anomalies at similar depths below this subduction zone (e.g., Jaxybulatov et al. 2013).

3.3. The Peru Area

This area is characterised by the subduction of the Nazca Plate beneath the South America Plate. Two pronounced later arrivals are observed in one record section recorded at the USArray in north America, and we detect two anomalies at depths of 1150 km and 1500 km below the source in the Peru area (Fig. 7).

4. Discussion

4.1. The Seismic Property of Scatterers

A 7 km-thick LVL structure with shear-wave velocity and density change by −4% and +5%,

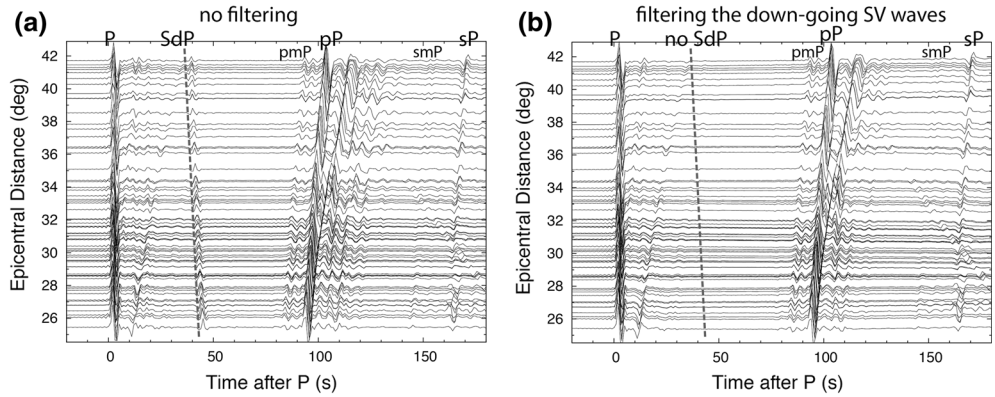

Figure 3
Synthetic section comparison between **a**full-wave fields modelling with **b** filtering the down-going SV waves for the 2010 July 23 event. Note that source-sided Moho underside reflections (pmP and smP) are also noticeable in the synthetic sections

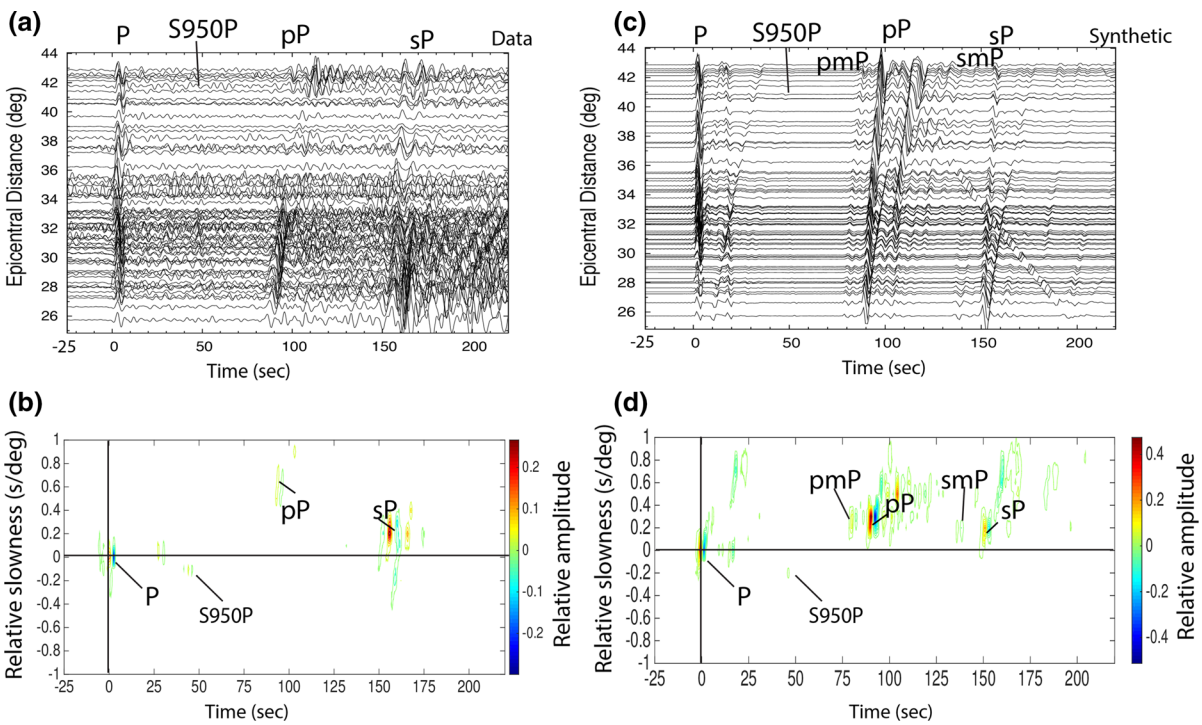

Figure 4
a Seismic record section and **b** fourth root vespagram for the 2005 Feb. 5 event. **c** Corresponding synthetic seismograms computed in a modified IASPEI91 model, in which a 7 km-thick low-velocity layer is embedded at 950 km depth. **d** The velocity vespagram for the synthetic section. A scatterer at ∼950 km depth below the source is detected in the eastern Indonesia, and slightly deviates from the great-circle direction to the east by ∼100 km as constrained by the beam-forming analysis (Fig. 2). Note that the amplitudes of synthetic waveforms are slightly lower than the observations

respectively, can adequately explain the observed SdP arrivals in terms of arrival-time, slowness, and relative amplitude (Figs. 4, 5, 6, and 7), although a dipping geometry of the reflector may cause uncertainties. We acknowledge that it is a big challenge to constrain the dipping geometry together with the seismic contrast until a 3-D modelling is performed in a future study, and our efforts in this

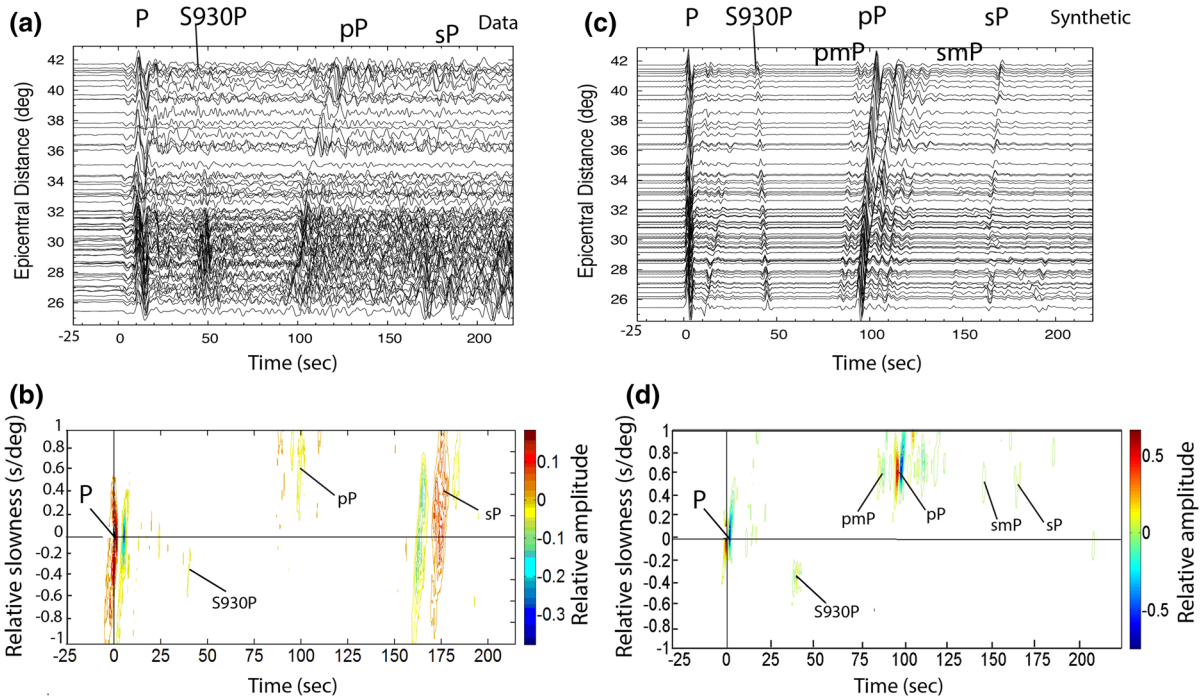

Figure 5

Same caption as Fig. 4, but for the 2010 July 23 event. A scatterer at a depth of 930 km, deviating from the great-circle direction to the west by ~400 km, is detected. It is worth noting that the synthetic modelling explains the data for the SdP phase adequately

study are primarily to demonstrate the existence of a number of scatterers in the mid-mantle beneath subduction zones and discuss the possible properties of those slow anomalies in light of existing explanations (e.g., Niu et al. 2003; Yang and He 2015). Although some discrepancies may exist between the data and synthetics, perhaps, due to a dipping geometry, but the analyses of the differential travel-times of P versus SdP (Fig. 8) show that a flat structure can adequately explain the observations, occasionally even better than a dipping geometry, and a horizontal layer can hence be of first-order estimation.

4.2. *Comparison to Other Studies*

In the eastern Indonesia area, the previous SdP studies have reported three scatterers in existence at ~910 km (Yang and He 2015), ~930 km, and ~970 km (Vanacore et al. 2006) in the mid-mantle. All evidences together suggest that such small-scale structures are clustered at depths ranging from ~910 to ~970 km in this region. These heterogeneities are probably related to the fragments of subducted Proto-South China Sea slab as seen by tomographic imaging (Hall 2002; Hall and Spakman 2015). The presence of 4 scatterers at various depths likely reflects a severe fragmentation history of the slab encountering with the mid-mantle.

In the Izu–Bonin region, similar results show scatterers in the mid-mantle of the Izu–Bonin area via a variety of approaches such as P-to-P scattering (e.g., Bentham and Rost 2014) and S-to-P conversion (e.g., Castle and Creager 1999). It is worth noting that, in the Mariana region (e.g., Castle and van der Hilst 2003; Korenaga 2015), the scatterers have been detected to ~2000 km depth, which is so far the deepest observation relevant to SdP waves along various subduction systems.

In the Peru area, two anomalies at depths of 1150 km and 1500 km below the source are detected (Fig. 7). Our observations are consistent with previous studies (Kaneshima and Helffrich 2010) for S-to-P scattering energy at the mid-lower mantle depths.

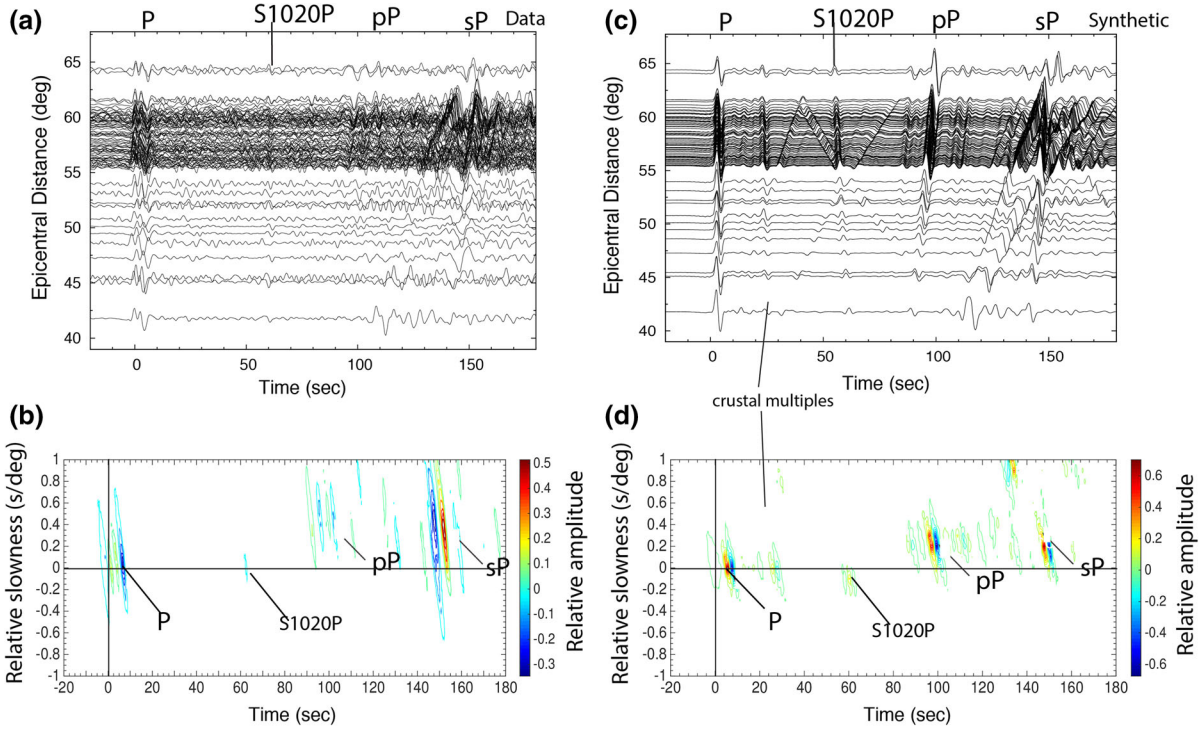

Figure 6
Same caption as Fig. 4, but for the 2015 June 23 event. A scatterer at a depth of 1020 km is detected below the source. Note that the synthetic SdP waveform here displays high similarity compared to the data

The scattering signals are probably related to fragments of subducted Farallon plate as seen a positive anomaly in the previous tomographic models (e.g., Ren et al. 2007).

Our suggestion here is also consistent with a previous seismic observation revealing that this compositionally distinct layer is thought to have higher density and lower versus relative to the surrounding mantle (Niu 2014). In addition, basaltic crust is characterised by ~7 km thickness in nature, which is compatible with the layer resolved by the signal of S-to-P with dominant frequency up to 0.5 Hz in this study. All behaviours agree with inferences from a calculation of mineral physics for elasticity of oceanic crust in an MORB composition (Tsuchiya 2011). This basaltic heterogeneity has also been detected by other seismic energies like PP precursors (e.g., Rost et al. 2008; Bentham and Rost 2014; Bentham et al. 2017), SS precursors (e.g., Petersen et al. 1993; Deuss and Woodhouse 2002; Gu et al. 2012), and multiple ScS reverberations (Courtier and Revenaugh 2008). Various approaches together suggest a direct causal link between seismic short-wavelength heterogeneities in the mid-mantle with past subducted oceanic crust, which has been likely separated from its accompanying lithosphere (e.g., Richards and Davies 1989; van Keken et al. 1996; Karato 1997; Lee and Chen 2007; Yang and He 2015).

The quite different depths of scatterers in the three regions can happen if separation of crustal component from subducted slab occurred at different depths, which may be associated with various interaction processes between slab and surrounding mid-mantle.

4.3. The Fate and Recycling of Basaltic Crust

Combined with the results from previous studies, the oceanic crust in the mid-mantle appears to pool at the depths ranging from ~700 to 1110 km with a few deeper penetrations into depth of ~1600 km beneath the Marianas region (e.g.,

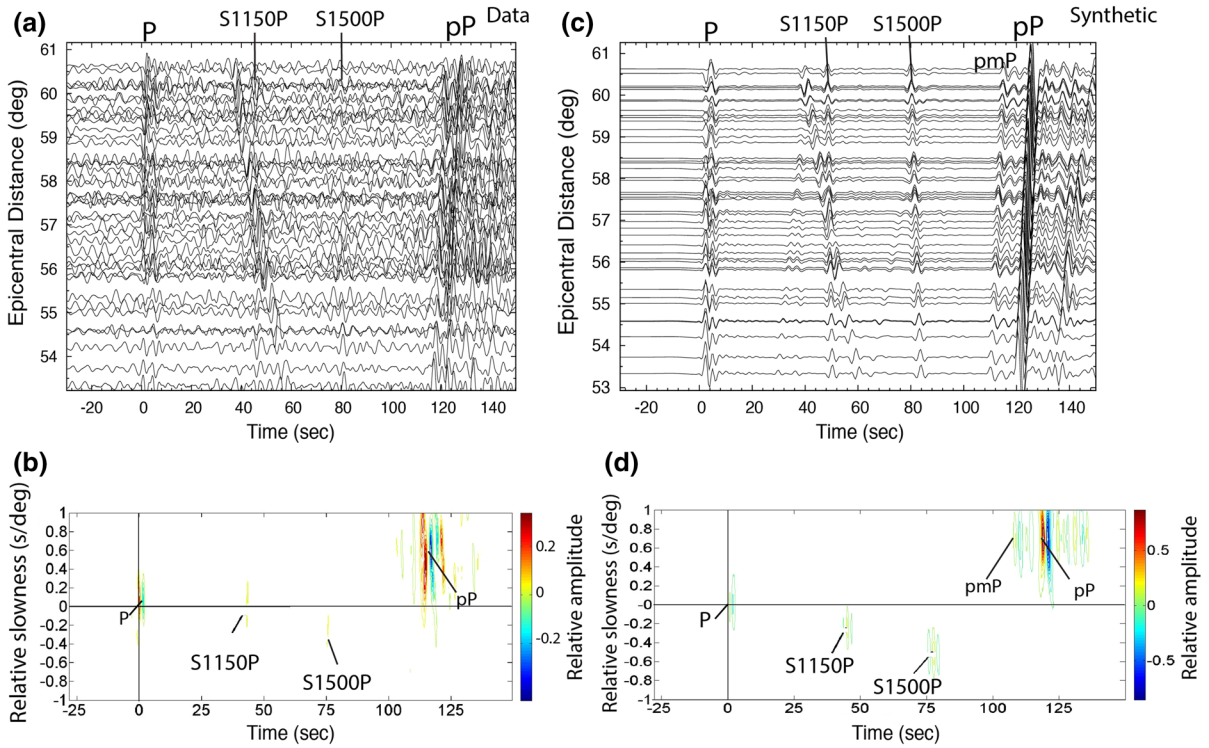

Figure 7
Same caption as Fig. 4, but for the 2007 July 21 event. Two scatterers at a depth of 1150 and 1500 km are detected below the source. The synthetics through an unperturbed IASP91 is presented in Figure S4 of supplementary materials, allowing an interpretation of the influence of the heterogeneous model

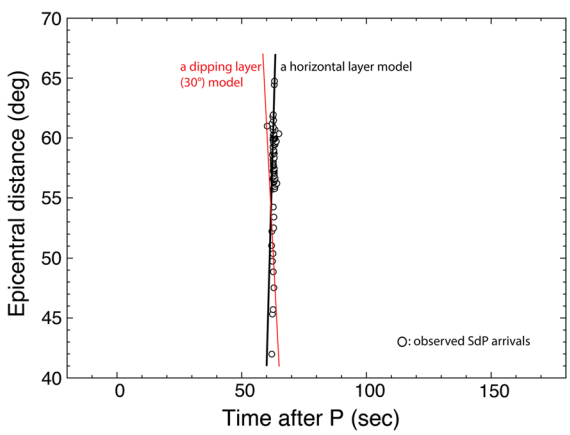

Figure 8
Plot for SdP travel-times relative to P as a function of epicentral distances for the 2015 June 23 event, in which open circles denote the observed SdP arrival-times after P waves, and black and red lines represent the reduced arrival-time curves for a horizontal layer and a dipping layer (with a dipping angle of 30°), respectively. In this case, the dipping model does not explain the observations better compared to a flat structure

Castle and van der Hilst 2003; Korenaga 2015). Slab stagnation in the mid-mantle has been explained experimentally by mineral physics studies, revealing that the viscosity in the mid-mantle is strongly increased and controlled by ferropericlase (main constituents of the lower mantle) (Marquardt and Miyagi 2015). This phenomena of viscosity jump in the Earth's mid-mantle was confirmed subsequently by reanalysing the long-wavelength nonhydrostatic geoid (Rudolph et al. 2015). And accordingly, we suggest that the oceanic crust has been trapped substantially in the mid-mantle, at least temporarily, before it accumulates at the base of the lower mantle beneath subduction zones eventually. The S-to-P energy is thought to be generated at oceanic crust in the mid-mantle and stagnating due to viscosity increase as a result of a spin transition in ferropericlase (e.g., Justo et al. 2015; Shahnas et al. 2017a, b). It is worth noting

that an alternative model by introducing bridgmanite-enriched ancient mantle structures in the lower mantle seems promising to explain slab stagnation in the mid-mantle (Ballmer et al. 2015, 2017).

The fate of basaltic crust might differ from that of the underlying peridotite layer because of differences in chemistry, density, and melting temperature. It has been speculated that subducted basaltic crust may be gravitationally trapped at depths of at least 800 km (e.g., Irifune and Ringwood 1993), whereas the subsequent mineral physics analysis revealed that the former MORB material is denser than the average lower mantle at all depths greater than ~720 km (e.g., Hirose et al. 1999). The subducted basaltic crust may, therefore, have accumulated either above the 660 km boundary, or at the base of mantle. Basaltic accumulation in the transition zone (TZ) has been confirmed by high-frequency seismic observations from a global data set (e.g., Shen et al. 2014), and its signature via recycling from the TZ has been seen in the geochemical signals from analysing samples of continental basalts (e.g., Li et al. 2015). Basaltic accumulation at the base of the mantle is also consistent with geochemical inference (e.g., Christensen and Hofmann 1994), and its recycling from D" layer is suspected to feed hotspots (e.g., Hofmann 1997) and results in their chemical complexity (e.g., Li et al. 2014). Therefore, combined with observations in the mid-mantle, oceanic crust exhibits a wide range of depths from the TZ to the base of the mantle. It is worth noting that a thermodynamic computation also suggested an increase of basalt fraction with depth in the mantle (Xu et al. 2008). In addition, recent receiver functions study beneath Western Europe suggested that such mid-mantle seismic features are not unique to subduction zones (Jenkins et al. 2017), reflecting a possible existence of global signature.

5. Conclusion

In summary, we observe a prominent arrival of SdP after the direct P wave in the recordings of F-net, the Alaska network, and the USArray. Our analyses reveal that four compositional distinct low-velocity layers are most likely relevant to the past subducted oceanic crust at various depths in the mid-mantle, where viscosity has considerably increased. The SdP arrival is increasingly proven to be a very useful signal to explore such deep, short-wavelength compositional structures.

Acknowledgements

We gratefully acknowledge IRIS and F-net for making waveform data available. Figures were made with GMT (Wessel and Smith 1995) and GNUPLOT. We thank Prof. Wim Spakman (editor), Dr. Sebastian Rost, and three anonymous reviewers for the careful and constructive review comment. This work was supported by the National Science Foundation of China (Grants 91428309, 41761134051) and State Key Laboratory of Marine Geology, Tongji University (No. MGK1705).

References

Ballmer, M. D., Schmerr, N. C., Nakagawa, T., & Ritsema, J. (2015). Compositional mantle layering revealed by slab stagnation at 1000-km depth. *Science Advances*, *1*(11), e1500815. https://doi.org/10.1126/sciadv.1500815.

Ballmer, M. D., Houser, C., Hernlund, J. W., Wentzcovitch, R. M., & Hirose, K. (2017). Persistence of strong silica-enriched domains in the Earth's lower mantle. *Nature Geoscience*, *10*(3), 236–240. https://doi.org/10.1038/NGEO2898.

Bentham, H., & Rost, S. (2014). Scattering beneath western Pacific subduction zones: evidence for oceanic crust in the mid-mantle. *Geophysical Journal International*, *197*, 1627–1641.

Bentham, H. L. M., Rost, S., & Thorne, M. S. (2017). Fine-scale structure of the mid-mantle characterised by global stacks of PP precursors. *Earth and Planetary Science Letters*, *472*, 164–173.

Castle, J. C., & Creager, K. C. (1999). A steeply dipping discontinuity in the lower mantle beneath Izu-Bonin. *Journal of Geophysical Research: Solid Earth*, *104*(B4), 7279–7292.

Castle, J. C., & van der Hilst, R. D. (2003). Searching for seismic scattering off mantle interfaces between 800 km and 2000 km depth. *Journal of Geophysical Research: Solid Earth*, *108*(B2), 2095. https://doi.org/10.1029/2001JB000286.

Courtier, A. M., & Revenaugh, J. (2008). Slabs and shear wave reflectors in the midmantle. *Journal of Geophysical Research: Solid Earth*, *113*, B08312. https://doi.org/10.1029/2007JB005261.

Christensen, U. R., & Hofmann, A. W. (1994). Segregation of subducted oceanic crust in the convecting mantle. *Journal of Geophysical Research: Solid Earth*, *99*(B10), 19867–19884.

Deuss, A., & Woodhouse, J. H. (2002). A systematic search for mantle discontinuities using SS-precursors. *Geophysical*

Research Letters, *29*(8), 1249. https://doi.org/10.1029/2002GL014768.

Dziewonski, A. M., & Woodhouse, J. H. (1987). Global images of the Earths interior. *Science*, *236*, 37–48.

French, S. W., & Romanowicz, B. (2015). Broad plumes rooted at the base of the Earth's mantle beneath major hotspots. *Nature*, *525*, 95–99.

Fukao, Y., & Obayashi, M. (2013). Subducted slabs stagnant above, penetrating through, and trapped below the 660 km discontinuity. *Journal of Geophysical Research: Solid Earth*, *118*(11), 5920–5938.

Gu, Y. J., Okeler, A., & Schultz, R. (2012). Tracking slabs beneath northwestern Pacific subduction zones. *Earth and Planetary Science Letters*, *331–332*, 269–280. https://doi.org/10.1016/j.epsl.2012.03.023.

Hall, R. (2002). Cenozoic geological and plate tectonic evolution of SE Asia and the SW Pacific: computer-based reconstructions, model and animations. *Journal of Asian Earth Sciences*, *20*, 353–434.

Hall, R., & Spakman, W. (2015). Mantle structure and tectonic history of SE Asia. *Tectonophysics*, *658*, 14–45.

Hedlin, M. A. H., Shearer, P. M., & Earle, P. S. (1997). Seismic evidence for small-scale heterogeneity throughout the Earths mantle. *Nature*, *387*, 145–150.

Helffrich, G. (2006). Heterogeneity in the mantle; its creation, evolution and destruction. *Tectonophysics*, *416*(1–4), 23–31.

Hirose, K., Fei, Y., Ma, Y., & Mao, H.-K. (1999). The fate of subducted basaltic crust in the Earths lower mantle. *Nature*, *397*, 53–56.

Hofmann, A. W. (1997). Mantle geochemistry: the message from oceanic volcanism. *Nature*, *385*(6613), 219–229.

Irifune, T., & Ringwood, A. E. (1993). Phase transformations in subducted oceanic crust and buoyancy relationships at depths of 600–800 km in the mantle. *Earth and Planetary Science Letters*, *117*, 101–110.

Jaxybulatov, K., Koulakov, I., & Dobretsov, N. L. (2013). Segmentation of the Izu-Bonin and Mariana slabs based on the analysis of the Benioff seismicity distribution and regional tomography results. *Solid Earth*, *4*, 59–73. https://doi.org/10.5194/se-4-59-2013.

Jenkins, J., Deuss, A., & Cottaar, S. (2017). Converted phases from sharp 1000 km depth mid-mantle heterogeneity beneath Western Europe. *Earth and Planetary Science Letters*, *459*, 196–207.

Justo, J. F., Morra, G., & Yuen, D. A. (2015). Viscosity undulations in the lower mantle: The dynamical role of iron spin transition. *Earth and Planetary Science Letters*, *421*, 20–26.

Kaneshima, S. (2003). Small-scale heterogeneity at the top of the lower mantle around the Mariana slab. *Earth and Planetary Science Letters*, *209*, 85–101.

Kaneshima, S. (2009). Seismic scatterers at the shallowest lower mantle beneath subducted slabs. *Earth and Planetary Science Letters*, *286*, 304–315.

Kaneshima, S., & Helffrich, G. (2010). Small scale heterogeneity in the mid- lower mantle beneath the circum-Pacific area. *Physics of the Earth and Planetary Interiors*, *183*, 91–103.

Kaneshima, S. (2016). Seismic scatterers in the mid-lower mantle. *Physics of the Earth and Planetary Interiors*, *257*, 105–114.

Karato, S.-I. (1997). On the separation of crustal component from subducted oceanic lithosphere near the 660 km discontinuity. *Physics of the Earth and Planetary Interiors*, *99*, 103–111.

Kawakatsu, H., & Niu, F. (1994). Seismic evidence for a 920-km discontinuity in the mantle. *Nature*, *371*, 301–305.

Korenaga, J. (2015). Constraining the geometries of small-scale heterogeneities: A case study from the Mariana region. *Journal of Geophysical Research: Solid Earth*, *120*(11), 7830–7851. https://doi.org/10.1002/2015JB012432.

Kennett, B. L. N., & Engdahl, E. R. (1991). Travel times for global earthquake location and phase identification. *Geophysical Journal International*, *105*, 429–465.

Lee, C.-T. A., & Chen, W.-P. (2007). Possible density segregation of subducted oceanic lithosphere along a weak serpentinite layer and implications for compositional stratification of the Earth's mantle. *Earth and Planetary Science Letters*, *255*, 357–366.

Li, M., NcNamara, A. K., & Garnero, E. J. (2014). Chemical complexity of hotspots caused by cycling oceanic crust through mantle reservoirs. *Nature Geoscience*, *7*, 366–370. https://doi.org/10.1038/ngeo2120.

Li, J., & Yuen, D. A. (2014). Mid-mantle heterogeneities associated with Izanagi plate: implications for regional mantle viscosity. *Earth and Planetary Science Letters*, *385*, 137–144.

Li, Y.-Q., Ma, C.-Q., Robinson, P. T., Zhou, Q., & Liu, M.-L. (2015). Recycling of oceanic crust from a stagnant slab in the mantle transition zone: Evidence from Cenozoic continental basalts in Zhejiang Province, SE China. *Lithos*, *230*, 146–165.

Mancinelli, N., & Shearer, P. (2016). Scattered energy from a rough core-mantle boundary modeled by a Monte Carlo seismic particle method: Application to PKKP precursors. *Geophysical Research Letters*, *43*(15), 7963–7972. https://doi.org/10.1002/2016GL070286.

Marquardt, H., & Miyagi, L. (2015). Slab stagnation in the shallow lower mantle linked to an increase in mantle viscosity. *Nature Geoscience*, *8*, 311–314. https://doi.org/10.1038/ngeo2393.

Niu, F., Kawakatsu, H., & Fukao, Y. (2003). Seismic evidence for a chemical heterogeneity in the midmantle: a strong and slightly dipping seismic reflector beneath the Mariana subduction zone. *Journal of Geophysical Research: Solid Earth*, *108*, 1978–2012.

Niu, F. (2014). Distinct compositional thin layers at mid-mantle depths beneath northeast China revealed by the USArray. *Earth and Planetary Science Letters*, *402*, 305–312.

Petersen, N., Gossler, J., Kind, R., Stammler, K., & Vinnik, L. (1993). Precursors to SS and structures of transition zone of the North-Western Pacific. *Geophysical Research Letters*, *20*(4), 281–284.

Ren, Y., Stulzmann, E., van der Hilst, R. D., & Besse, J. (2007). Under- standing seismic heterogeneities in the lower mantle beneath the Americas from seismic tomography and plate tectonic history. *Journal of Geophysical Research: Solid Earth*, *112*, B01302. https://doi.org/10.1029/2005JB004154.

Rost, S., & Thomas, C. (2002). Array seismology: methods and applications. *Reviews of Geophysics*, *40*(3), 1008. https://doi.org/10.1029/2000RG000100.

Rost, S., Garnero, E. J., & Williams, Q. (2008). Seismic array detection of subducted oceanic crust in the lower mantle. *Journal of Geophysical Research: Solid Earth*, *113*, B06303. https://doi.org/10.1029/2007JB005263.

Richards, M. A., & Davies, G. F. (1989). On the separation relatively buoyant components from subducted lithosphere. *Geophysical Research Letters*, *16*(8), 831–834.

Rudolph, M. L., Lekić, V., & Lithgow-Bertelloni, C. (2015). Viscosity jump in Earth's mid-mantle. *Science*, *350*(6266), 1349–1352. https://doi.org/10.1126/science.aad1929.

Shahnas, M. H., Yuen, D. A., & Pysklywec, R. N. (2017). Mid-mantle heterogeneities and iron spin transition in the lower mantle: Implications for mid-mantle slab stagnation. *Earth and Planetary Science Letters*, *458*, 293–304.

Shahnas, M. H., Pysklywec, R. N., Justo, J. F., & Yuen, D. A. (2017). Spin transition-induced anomalies in the lower mantle: implications for mid-mantle partial layering. *Geophysical Journal International*, *210*, 765–773.

Shen, X., Yuan, X., & Li, X. (2014). A ubiquitous low-velocity layer at the base of the mantle transition zone. *Geophysical Research Letters*, *41*, 836–842.

Tsuchiya, T. (2011). Elasticity of subducted basaltic crust at the lower mantle pressures: insights on the nature of deep mantle heterogeneity. *Physics of the Earth and Planetary Interiors*, *188*, 142–149.

Vanacore, E., Niu, F., & Kawakatsu, H. (2006). Observations of the mid-mantle discontinuity beneath Indonesia from S to P converted waveforms. *Geophysical Research Letters*, *33*, L04302. https://doi.org/10.1029/2005GL025106.

van Keken, P. E., Karato, S., & Yuen, D. A. (1996). Rheological control of oceanic crust separation in the transition zone. *Geophysical Research Letters*, *23*(14), 1821–1824.

Wang, R. (1999). A simple orthonormalization method for stable and efficient computation of Greens functions. *Bulletin of the Seismological Society of America*, *89*, 733–741.

Waszek, L., Thomas, C., & Deuss, A. (2015). PKP precursors: Implications for global scatterers. *Geophysical Research Letters*, *42*(10), 3829–3838. https://doi.org/10.1002/2015GL063869.

Wessel, P., & Smith, W. H. F. (1995). New version of the generic mapping tools. *Eos, Transactions American Geophysical Union*, *76*(33), 329. https://doi.org/10.1029/95EO00198.

Xu, W., Lithgow-Bertelloni, C., Stixrude, L., & Ritsema, J. (2008). The effect of bulk composition and temperature on mantle seismic structure. *Earth and Planetary Science Letters*, *275*, 70–79.

Yang, Z., & He, X. (2015). Oceanic crust in the mid-mantle beneath West-Central Pacific subduction zones: Evidence from S to P converted waveforms. *Geophysical Journal Internationa*, *203*(1), 541–547. https://doi.org/10.1093/gji/ggv314.

(Received October 26, 2016, revised December 1, 2017, accepted December 19, 2017)